Title	Photoelectronic Responses in Solution-Processed Perovskite CH[3]NH[3]PbI[3] Solar Cells Studied by Photoluminescence and Photoabsorption Spectroscopy
Author(s)	Yamada, Yasuhiro; Nakamura, Toru; Endo, Masaru; Wakamiya, Atsushi; Kanemitsu, Yoshihiko
Citation	IEEE Journal of Photovoltaics (2015), 5(1): 401-405
Issue Date	2015-01
URL	http://hdl.handle.net/2433/193280
Right	© 2014 IEEE. Personal use of this material is permitted. Permission from IEEE must be obtained for all other uses, in any current or future media, including reprinting/republishing this material for advertising or promotional purposes, creating new collective works, for resale or redistribution to servers or lists, or reuse of any copyrighted component of this work in other works.
Type	Journal Article
Textversion	author

Photoelectronic responses in solution-processed perovskite $CH_3NH_3PbI_3$ solar cells studied by photoluminescence and photoabsorption spectroscopy

Yasuhiro Yamada, Toru Nakamura, Masaru Endo, Atsushi Wakamiya, and Yoshihiko Kanemitsu

***Abstract*— Photoelectronic responses of organic-inorganic hybrid perovskite $CH_3NH_3PbI_3$ on mesoporous TiO_2 electrodes are investigated. On the basis of near-band-edge optical absorption and photoluminescence spectra, the bandgap energy and exciton binding energy as a function of temperature are obtained. The exciton binding energy is much smaller than thermal energy at room temperature, which means that most excitons are thermally dissociated and optical processes are determined by the photoexcited electrons and holes. We determined the temperature dependence of exciton binding energy, which changes from ~30 meV at 13 K to 6 meV at 300 K. In addition, the bandgap energy and the exciton binding energy show abrupt changes at 150 K due to structural phase transition. Our fundamental optical studies provide essential information for improving the device performance of solar cells based on halide perovskite semiconductors.**

***Index Terms*— Photoluminescence, Semiconductor devices, Solar energy**

I. Introduction

Lead halide perovskites, $CH_3NH_3PbX_3$ [X = Cl, Br, and I], have recently emerged as a promising candidate material for efficient light-energy conversion devices. Although $CH_3NH_3PbX_3$ itself is a three-dimensional semiconductor, organic-inorganic hybrid lead halide perovskite semiconductors have previously been examined extensively with regards to the unique optical properties of natural lower-dimensional layered perovskite-type compounds [1],[2]. In 2009, Kojima *et al*. [3] first reported the development of a sensitized solar cell using perovskite $CH_3NH_3PbI_3$ as a light-harvesting sensitizer with mesoporous TiO_2 electrodes and liquid electrolyte. The further breakthrough was the realization of an efficient all-solid-state sensitized solar cell with power conversion efficiency above 10 % based on perovskite $CH_3NH_3PbI_3$, with the use of the solid-state hole-transporting material Spiro-OMeTAD [4],[5]. With ongoing research, the power conversion efficiency of perovskite-based devices has improved rapidly and is currently at over 19 % [2]-[10], which is much higher than that of conventional dye-sensitized solar cells. More recently, the planar heterojunction-type perovskite solar cell has also been developed [11],[12].

In order to further contribute to the development of increasingly efficient perovskite solar cells, it is necessary to identify the key mechanism that determines the advanced photovoltaic properties of perovskite semiconductors. To date, it has been demonstrated that long carrier diffusion length contributes to the high efficiency of these solar cells [13],[14]. The estimation of diffusion length was conducted using time-resolved photoluminescence (PL) spectroscopy in perovskite thin films, assuming the one-dimensional exciton diffusion model. However, it has not been clarified whether the exciton or free carrier mechanism is an appropriate interpretation of the optical properties. To answer this question, we need to evaluate the exciton binding energy of $CH_3NH_3PbI_3$. Although several researches have been made to evaluate the exciton binding energy of $CH_3NH_3PbI_3$ bulk crystals and thin films, the reported literature values are scattered over a wide range [15]-[18], and it still remains under discussion. Therefore, in order to promote an improved understanding of the intrinsic characteristics of perovskite solar cells, it is necessary to reveal fundamental optical properties of perovskite semiconductors and evaluate the exciton binding energy.

In our previous report, we obtained the room-temperature bandgap energy of $CH_3NH_3PbI_3$ on mesoporous TiO_2 electrodes based on their PL, PL excitation, and transient absorption [19]. The combination of these different optical spectroscopy techniques provides detailed information on optical properties [20],[21]. It was found that the PL and PLE spectra have peaks at 1.60 and 1.64 eV, respectively, and we observed a negative TA peak at 1.61 eV due to photobleaching, which usually appears at the bandgap energy of direct bandgap semiconductors. We therefore determined that the direct bandgap energy is 1.61 eV at room temperature.

In this paper, we discuss the optical absorption spectra measured through total optical transmittance (TT) and diffuse reflectance (DR) analyses in a wide temperature range. The

This paragraph of the first footnote will contain the date on which you submitted your paper for review.

Y. Yamada, M. Endo, A. Wakmiya, and Y. Kanemitsu are with Institute for Chemical Research, Kyoto University, Uji, Kyoto, 611-0011 JAPAN (e-mail: yamada.yasuhiro.6c@kyoto-u.ac.jp; endo@hydrogen.kuicr.kyoto-u.ac.jp; wakamiya@scl.kyoto-u.ac.jp; kanemitu@scl.kyoto-u.ac.jp).

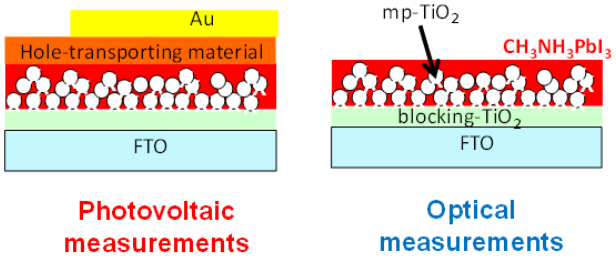

Fig. 1. Schematic illustration of the perovskite solar cells and samples. Optical measurements were performed on the sample without hole transporting material and gold electrode. The $CH_3NH_3PbI_3$ layer was formed on the mesoporous TiO_2 electrode.

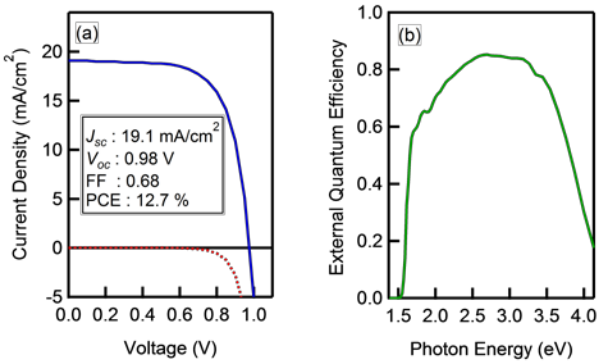

Fig. 2. (a) Current-density–voltage curves under illumination (solid curve) and in the dark (broken curve) and (b) external quantum efficiency spectrum of our perovskite solar cell.

fabrication process of the perovskite thin films and perovskite-based solar cells used in this study is outlined. The optical absorption spectra of these samples are then obtained and analyzed, taking excitonic effects into consideration, and the temperature dependence of the bandgap energy, the exciton binding energy, and the broadening parameter are determined. Temperature-dependent PL spectra are also measured.

II. Samples and Experimental Setup

Perovskite thin films were fabricated on mesoporous TiO_2 electrodes using the two-step method [8]. The porous TiO_2 layer was deposited on the glass substrate through spin coating using a TiO_2 paste. The porous TiO_2 films were infiltrated with PbI_2 (99.999%, Sigma-Aldrich) through the spin-coating of a PbI_2 solution in N,N-dimethylformamide in an argon-filled glove box. After maintaining a temperature of 70 °C for 30 min to allow the material to dry, the films were dipped in a solution of CH_3NH_3I in 2-propanol and then rinsed with 2-propanol. We then conducted optical measurements on these samples. Perovskite-based photovoltaic cells were also fabricated by attaching hole-transporting material and gold electrodes to the samples (see [19] and [22] for this fabrication method). The structures of the samples used in the optical and photovoltaic measurements are illustrated schematically in Fig. 1. Before and during the experiment, the samples were maintained in an argon atmosphere to avoid degradation due to air exposure. In addition, the samples were left for more than three days after fabrication to allow the intrinsic material properties to stabilize.

To evaluate the near-band-edge optical properties, we measured total optical transmittance, which is the angle-integrated intensity of forward scattered light, using an integrating sphere because of the strong light-scattering due to the mesoporous TiO_2. In addition, DR spectroscopy was used to obtain temperature-dependent optical absorption spectra. The acquired DR spectrum was converted to the Kubelka-Munk function F(R), which is approximately proportional to the absorption coefficient, according to the relation $F(R) = (1-R)^2/(2R)$, where R is the diffuse reflectivity. PL measurements were performed using a Si CCD camera with a monochromator.

III. Results and Discussion

We confirmed that the solar cell with the produced $CH_3NH_3PbI_3$ works well, particularly with regards to power-conversion efficiency. Fig. 2 shows the solar-cell performance of our perovskite-based solar cell. We estimated the power conversion efficiency under AM 1.5 conditions. It shows high open-circuit voltage (V_{OC} = 0.98 V), short-circuit current (J_{SC} = 19.1 mA/cm^2), and fill-factor (FF = 0.68). The power-conversion efficiency was 12.7 %.

To evaluate the optical properties of $CH_3NH_3PbI_3$, we conducted optical absorption measurements as shown in Fig. 3. While DR measurement of perovskite solar cells has been conducted previously [5],[6],[19], we also carried out total transmittance (TT) measurement to achieve a more accurate optical absorption spectrum. For comparison, the DR spectrum is normalized and offset, and it was found that the TT and DR spectra were in good agreement with each other. However, the TT spectra had less signal-to-noise ratio compared with the DR measurements. Therefore, the TT spectra were used for analysis of the perovskite solar cell properties at room temperature.

As we have stated previously, $CH_3NH_3PbI_3$ is a direct-gap semiconductor [19]. Its TT spectrum has no excitonic peaks, suggesting the exciton binding energy is much smaller than the thermal energy at room temperature (~25 meV). However, even in this case, it is known that the near-band-edge optical absorption is modified due to excitonic effects [23]-[25]. According to [23] and [24], the near-band-edge optical absorption spectrum for a dipole-allowed direct-gap semiconductor, taking excitonic effects into consideration, is expressed as

$$\alpha \propto A\sum_{n=1}^{\infty}\frac{1}{n^3}\delta(E-E_n)/E^2+\frac{(E-E_g)^{1/2}\tau e^{\tau}}{E\sinh\tau}, \quad (1)$$

where $\tau = \pi\left|E_b/(E-E_g)\right|$. E, E_g, and E_b are the photon energy, bandgap energy, and exciton binding energy, respectively. A is a proportionality coefficient that depends on temperature, while E_n is the exciton resonance energy and typically follows $E_n = E_g - E_b/n^2$ where n (= 1, 2, 3…) is the quantum number. The actual absorption spectrum is modified by intrinsic or extrinsic effects such as thermal broadening and

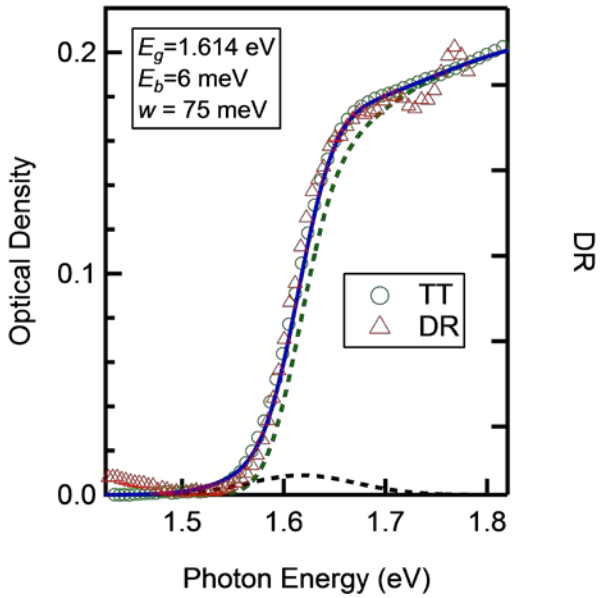

Fig. 3. (a) Optical absorption spectra obtained by total transmittance (circles) and diffuse reflectance (triangle) measurements. The solid curve is the fit given by Eqs. (1) and (2). The broken curve represents the Gaussian broadening function, $G(E)$, which is used in Eq. (2). We obtained w = 75 meV as a best fit parameter, which corresponds to the width of the Gaussian broadening function.

inhomogeneous broadening. To take these broadening effects into account, the optical absorption is convolved by the Gaussian broadening function $G(E)$, i.e.,

$$\alpha_r = \int_0^\infty \alpha(E)\, G(V-E)dV. \qquad (2)$$

We fit the TT spectra using (1) and (2). The fit result is shown in Fig. 3 as a solid curve, which conforms to the experimental data well, and the broadening function is given as a broken curve in the same figure. The obtained best fit parameters were E_g = 1.614 eV and E_b = 6 meV, while the broadening Gaussian function width (the broadening parameter), w = 75 meV. The estimated bandgap energy shows good agreement with our previous report. Note that the broadening parameter is much higher than the thermal energy at room temperature. We are of the view that this originates from the Urbach tail [19].

Based on the exciton binding energy result of 6 meV, we can conclude that the majority of the excitons in $CH_3NH_3PbI_3$ are thermally dissociated at room temperature. However, this exciton binding energy is much smaller than that given by previous reports, which had results in the range of 37 ~ 50 meV [15]-[17]. Since these values were estimated at low temperatures of approximately 10 K, we propose that the exciton binding energy varies with temperature. It has been reported that $CH_3NH_3PbI_3$ undergoes phase transition at 150 K and 330 K [19],[26] and large modification of optical properties is anticipated near the phase transition temperature [19].

To examine this suggestion, we conducted PL and DR measurements in a wide temperature range from 13 K to 300 K, as shown in Fig. 4. For the PL measurements, the excitation photon energy was 1.91 eV. At room temperature, the PL spectrum shows a broad peak at 1.60 eV. According to the estimated bandgap energy of 1.614 eV, there is only a small

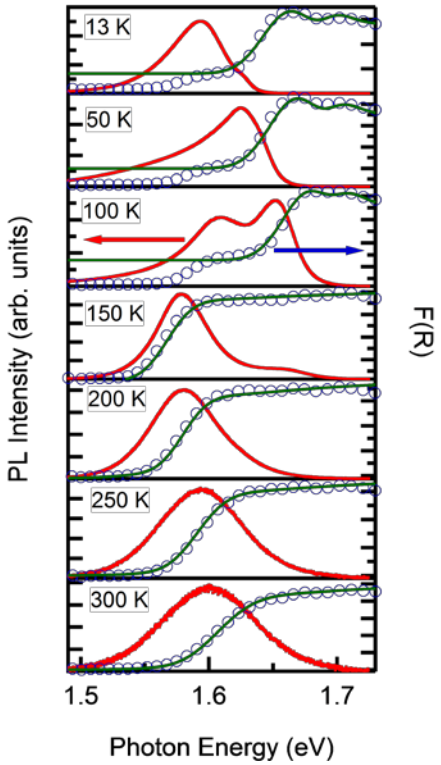

Fig. 4. PL and DR spectra at various temperatures. The solid curves represent the fit given by Eqs. (1) and (2). $F(R) = (1-R)^2/(2R)$, where R is the diffuse reflectivity.

Stokes shift and, therefore, we hold that the PL origin is the band-to-band radiative recombination of electrons at the conduction band and the holes at the valence band.

We confirmed that the PL spectrum shape is independent of excitation intensity and excitation photon energy under our experimental conditions. This means that the PL processes are independent of photoexcited carrier density. The low-temperature PL spectra are rather complicated: three PL components were observed. With a decrease in temperature, a new PL peak appears at approximately 1.65 eV and two-step optical absorption is observed. This is related to the structural phase transition in the region of this temperature [26]. We believe that the two phases coexist even below the phase transition temperature as, below 50 K, a new PL peak appears at 1.60 eV.

Regarding optical absorption spectra, a broad peak is observed near the band-edge in the optical absorption spectrum at low temperatures (below 50 K). It is our view that this broad peak corresponds to the n = 1 excitons. The DR spectra were fit using (1) and (2) and, at low temperatures (below 150 K) where two optical absorption edges coexist, we fit the high-energy absorption edge. The fit results are plotted as solid curves in Fig. 4. We obtained the bandgap energy, exciton binding energy, and broadening parameter as best-fit-parameters, which are indicated in Fig. 5. The bandgap energy and broadening parameter show abrupt changes at 150 K, the structural phase transition temperature. It can be seen that the broadening parameter gradually increases with temperatures above 150 K and the exciton binding energy is also temperature-dependent.

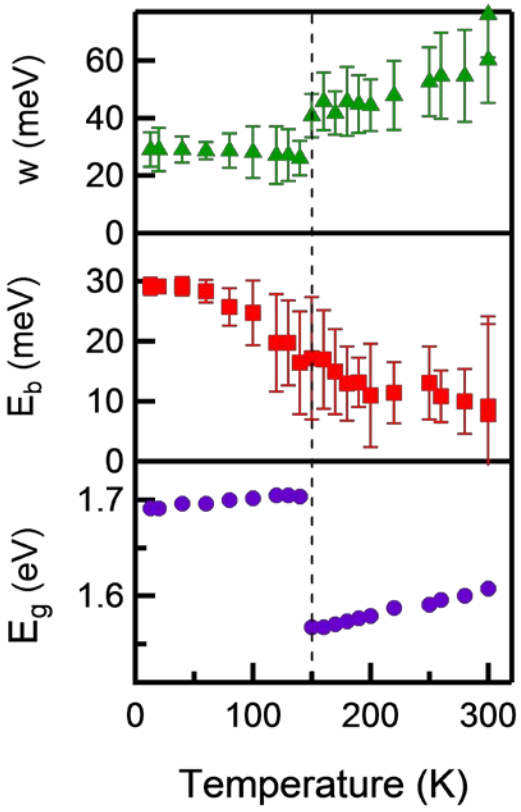

Fig. 5. Temperature dependence of the broadening parameter (w), exciton binding energy (E_b), and bandgap energy (E_g). The fitting errors for E_g were below 10 meV.

At 13 K, the estimated exciton binding energy is 30 meV, which is consistent with the previously reported value [15-17].

It is clear that the exciton binding energy decreases with temperature and a gradual change appears at the phase transition temperature. We hold that the temperature-dependent exciton binding energy can be explained by dielectric permittivity. The dielectric constant of $CH_3NH_3PbI_3$ should vary with temperature because of the phase transition temperature at 150 K and 330 K, and the exciton binding energy is inversely proportional to the square of the dielectric permittivity. In fact, it has been reported that the dielectric permittivity measured at 90 GHz increases with temperature above 150 K [27]. This trend is consistent with the observed temperature dependence of the exciton binding energy. In addition, it was pointed out that excitons are almost entirely screened at room temperature, yielding free carriers, due to optical phonons and collective rotational motion of the organic cations [28].

Our findings suggest that excitons in $CH_3NH_3PbI_3$ thin films are not stable at room temperature because of the smaller exciton binding energy (6 meV) than the thermal energy (25 meV), and photoexcited electrons and holes behave as free carriers. This result is consistent with our recent study on time-resolved PL and transient absorption which provides clear evidence that the radiative two-carrier recombination of free electrons and holes determines the optical processes in $CH_3NH_3PbI_3$ thin films [29].

Comparison with the previous reports should be mentioned. D'Innocenzo *et al.*, recently reported the exciton binding energy of 50 meV that were estimated from the temperature-dependence of exciton linewidth in optical absorption spectra above the phase transition temperature [18]. To estimate the exciton binding energy, they assumed the temperature-independent inhomogeneous linewidth. However, $CH_3NH_3PbI_3$ thin films show an increase of the bandgap energy with temperature above the phase transition temperature, and this trend is contrary to typical semiconductors, suggesting that material parameters in $CH_3NH_3PbI_3$ might change with temperature above the phase transition. On the other hand, we evaluated the exciton binding energy using whole spectrum shape near the bandgap energy without such an assumption. Based on these discussions, we believe that our estimation of exciton binding energy better accounts the near-band-edge optical properties of $CH_3NH_3PbI_3$. It is significant to employ various spectroscopic techniques to reveal the near-band-edge optical and excitonic properties of semiconductors. Through such researches, we can clarify the detailed mechanism for photovoltaic processes in emerging solar-cell materials, lead halide perovskites $CH_3NH_3PbX_3$ [X = Cl, Br, and I].

IV. Conclusion

In conclusion, we have studied the near-band-edge optical spectra of organic-inorganic hybrid perovskite $CH_3NH_3PbI_3$ on mesoporous TiO_2 electrodes by means of TT, DR, and PL measurements. At room temperature, no exciton peaks were observed in the optical absorption spectra. These spectra were then analyzed, taking excitonic effects into account, and an exciton binding energy of 6 meV was obtained. This result is much smaller than that given in previous reports estimated at low temperatures. This indicates that the exciton binding energy is temperature dependent. Further to this, we examined the temperature-dependent DR and PL spectra. At room temperature, almost no Stokes shift was observed. With a decrease in temperature, the exciton binding energy decreases and the PL peak and DR onset energy suddenly show a blue-shift at approximately 150 K, a structural phase transition temperature. We believe that our findings provide the requisite information to develop efficient perovskite solar cells.

Acknowledgment

This work was supported by The Sumitomo Electric Industries Group CSR foundation, JST-PRESTO, and JST-CREST.

References

[1] D. B. Mitzi, S. Wang, C. A. Feild, C. A. Chess, and A. M. Guloy, "Conducting Layered Organic-inorganic Halides Containing <110>-Oriented Perovskite Sheets," Science, vol. 267, pp. 1473-1476, Mar. 1995.

[2] T. Ogawa and Y. Kanemitsu, "Optical Properties of low-dimensional materials," (World Scientific, Singapore, 1995), Chap. 6.

[3] A. Kojima, K. Teshima, Y. Shirai, and T. Miyasaka," Organometal Halide perovskites as Visible-Light Sensitizers for Photovoltaic Cells," J. Am. Chem. Soc., vol. 131, pp. 6050–6051, Apr. 2009.

[4] J.-H. Im, C.-R. Lee, J.-W. Lee, S.-W. Park, and N.-G. Park, "6.5% efficient perovskite quantum-dot-sensitized solar cell," Nanoscale, vol. 3, pp. 4088-4093, Sep. 2011.

[5] H.-S. Kim, C.-R. Lee, J.-H. Im, K.-B. Lee, T. Moehl, A. Marchioro, S.-J. Moon, R. Humphry-Baker, J.-H. Yum, J. E. Moser, M. Grätzel, and N.-G. Park, "Lead Iodide Perovskite Sensitized All-Solid-State Submicron Thin Film Mesoscopic Solar Cell with Efficiency Exceeding 9%," Sci. Rep. vol. 2, pp. 591-1-591-7, Aug. 2012.

[6] M.M. Lee, J. Teuscher, T. Miyasaka, T. N. Murakami, H. J. Snaith, "Efficient Hybrid Solar Cells Based on Meso-Superstructured Organometal Halide Perovskites," Science, vol. 338, pp. 643-647, Nov. 2012.

[7] J.H. Heo, S.H. Im, J.H. Noh, T.N. Mandal, C.-S. Lim, J.A. Chang, Y.H. Lee, H.-J. Kim, A. Sarkar, M.K. Nazeeruddin, M. Grätzel and S.I. Seok, "Efficient inorganic–organic hybrid heterojunction solar cells containing perovskite compound and polymeric hole conductors," Nat. Photon., vol. **7**, pp. 486-491, May 2013.

[8] J. Burschka, N. Pellet, S.-J. Moon, R. Humphry-Baker, P. Gao, M. K. Nazeeruddin, and M. Grätzel, "Sequential deposition as a route to high-performance perovskite-sensitized solar cells," Nature, vol. 499, pp. 316-319, July 2013.

[9] P. Docampo, J. M. Ball, M. Darwich, G. E. Eperon, and H. J. Snaith, "Efficient organometal trihalide perovskite planar-heterojunction solar cells on flexible polymer substrates," Nat. Commun., Vol. 4, pp. 2761-1-2761-6, Nov. 2014.

[10] H. Zhou, Q. Chen, G. Li, S. Luo, T. Song, H. Duan, Z. Hong, J. You, Y. Liu, and Y. Yang, "Interface engineering of highly efficient perovskite solar cells", Science, vol. 345 pp. 542-546 Aug. 2014.

[11] M. Liu, M. B. Johnston, and H. J. Snaith, "Efficient planar heterojunction perovskite solar cells by vapour deposition," Nature, vol. 501, pp.395–398, Sep. 2013.

[12] G. E. Eperon, V. M. Burlakov, P. Docampo, A. Goriely, H. J. Snaith, "Morphological Control for High Performance, Solution-Processed Planar Heterojunction Perovskite Solar Cells," Adv. Func. Mater., vol. 24, pp. 151-157. Jan. 2014.

[13] S. D. Stranks, G. E. Eperon, G. Grancini, C. Menelaou, M. J. P. Alcocer, T. Leijtens, L. M. Herz, A. Petrozza, H. J. Snaith, "Electron-Hole Diffusion Lengths Exceeding 1 Micrometer in an Organometal Trihalide Perovskite Absorber", Science, vol. 342, pp. 341-344, Oct. 2013.

[14] G. Xing, N. Mathews, S. Sun, S. S. Lim, Y. M. Lam, M. Grätzel, S. Mhaisalkar, T. C. Sum, "Long-Range Balanced Electron- and Hole-Transport Lengths in Organic-Inorganic $CH_3NH_3PbI_3$," Science, vol. 342, pp. 344-347, Oct. 2013.

[15] T. Ishihara, "Optical properties of PbI-based perovskite structures," J. Lumin., vol. 60 – 61, pp. 269-274, Apr. 1994.

[16] M. Hirasawa, T. Ishihara, T. Goto, K. Uchida, N. Miura, "Magnetoabsorption of the lowest exciton in perovskite-type compound $(CH_3NH_3)PbI_3$," Physica B, vol. 201, pp. 427-431, July 1994.

[17] K. Tanaka, T. Takahashi, T. Ban, T. Kondo, K. Uchida, N. Miura, "Bandgap and exciton binding energies in lead-iodide-based natural quantum-well crystals," Solid State Commun., vol. 127, pp. 619–623, Sep. 2003.

[18] V. D'Innocenzo, G. Grancini, M.J.P. Alcocer, A.R.S. Kandada, S. D. Stranks, M. M. Lee, G. Lanzani, H. J. Snaith, and A. Petrozza, "Excitons versus free charges in organo-lead tri-halide perovskites," Nat. Comm. vol. 5 , pp 3586-1-3586-6, Aug. 2014.

[19]Y. Yamada, T. Nakamura, M. Endo, A. Wakamiya and Y. Kanemitsu, "Near-band-edge optical responses of solution-processed organic–inorganic hybrid perovskite $CH_3NH_3PbI_3$ on mesoporous TiO_2 electrodes," Appl. Phys. Express, vol. 7 pp.032302-1-032302-4, Mar. 2014.

[20] Y. Yamada and Y. Kanemitsu, "Determination of electron and hole lifetimes of rutile and anatase TiO_2 single crystals," Appl. Phys. Lett., vol. 101, pp. 133907-1- 133907-4, Sep. 2012.

[21] L. Q. Phuong, M. Okano, Y. Yamada, A. Nagaoka, K. Yoshino, and Y. Kanemitsu, "Photocarrier localization and recombination dynamics in Cu_2ZnSnS_4 single crystals," Appl. Phys. Lett., vol. 103, pp. 191902-1-191902-4, Nov. 2013.

[22] A. Wakamiya, M. Endo, T. Sasamori, N. Tokitoh, Y. Ogomi, S. Hayase, Y. Murata, "Reproducible Fabrication of Efficient Perovskite-based Solar Cells: X-ray Crystallographic Studies on the Formation of $CH_3NH_3PbI_3$ Layers," Chem. Lett., vol. 43 pp. 711-713, Feb. 2014.

[23] P. Y. Yu and M. Cardona, "Fundamentals of Semiconductors: Physics and Material Properties," 3rd ed. (Springer-Verlag, Berlin, 2005), Chap. 6.

[24] R. J. Elliott, "Intensity of Optical Absorption by Excitons." Phys. Rev., vol. 108, pp. 1384-1389, Dec. 1957.

[25] M.D. Sturge, "Optical Absorption of Gallium Arsenide between 0.6 and 2.75 eV," Phys. Rev., vol. 127, pp. 768-773, Aug. 1962.

[26] N. Onoda-Yamamuro, T. Matsuo, and H. Suga, "Calorimetric and IR spectroscopic studies of phase transitions in methylammonium trihalogenoplumbates (II)," J. Phys. Chem. Solids, vol. 51, pp. 1383-1395, July 1990.

[27] A. Poglitsch and D. Weber, "Dynamic disorder in methylammoniumtrihalogenoplumbates (II) observed by millimeterwave spectroscopy," J. Chem. Phys., vol. 87, pp. 6373-6378, Aug. 1987.

[28] J. Even, L. Pedesseau, and C. Katan, "Analysis of Multivalley and Multibandgap Absorption and Enhancement of Free Carriers Related to Exciton Screening in Hybrid Perovskites," J. Phys. Chem. C, vol. 118, pp. 11566-11572, May 2014.

[29] Y. Yamada, T. Nakamura, M. Endo, A. Wakamiya, and Y. Kanemitsu, "Photocarrier Recombination Dynamics in Perovskite $CH_3NH_3PbI_3$ for Solar Cell Applications," J. Am. Chem. Soc. vol. 136, pp 11610–11613, Aug. 2014.